Supporting Information

Ranieri et al. 10.1073/pnas.1008647107

SI Materials and Methods

Reagents and Antibodies. Most of the chemicals were obtained from Sigma-Aldrich. Rapamycin was from BIOMOL/Enzo Life Sciences; H2-DCF-DA was purchased from Invitrogen. Anti p66shc (cat. 07–150) and anti IRS-1 (cat. 06–248) polyclonal rabbit antisera were from Upstate Biotechnology/Millipore; anti-actin (goat polyclonal, cat. sc-1615 and sc-1616) and anti S6 kinase 1 (C18, sc-230) were from Santa Cruz Biotechnology; anti-HA mouse monoclonal antibody (HA.11, cat. MMS-101R) was from Covance; anti phosho-Ser-36 P66 shc (mouse monoclonal, clone 6E10) was from Alexis Biochemicals. All of the other antibodies (anti p-S6K1, Thr-389 cat. 9205; anti p-S6, Ser-235–236 cat. 2211; anti p-FKHRL1, Thr-32 cat. 9464; anti-phosho p44-42 MAP Kinase Thr202/Tyr204, cat 9101; anti phosho-(Ser-437) AkT, cat. 9271; anti AkT, cat. 9272; anti phospho IRS-1 (Ser-636–639) cat. 2388, anti phospho-(Ser-307) IRS-1, cat. 2381; anti phospho-(Thr-172) AMPK α cat. 2531; anti phospho (Thr-37–46) 4EBP1 cat. 2855; anti 4EBP1 cat. 9644; and anti phospho-(Thr-180-Tyr-182) p38MAPK were from Cell Signaling Technology.

Human recombinant insulin (Humulin, Eli Lilly was kindly provided from the pharmacy of the A. Gemelli Hospital, Catholic University, Rome. Human recombinant IGF1 was from Biodesign International. The Ultrasensitive (Mouse) Insulin Elisa kit (cat. 80-INSMSU-E01) was from Alpco immunoassays.

Plasmids, Cell Lines, and Transfections. The retroviral construct pBabe-Puro/p66shcA and the control construct encoding the green fluorescent protein in the same vector backbone were kindly provided by Prof. P. G. Pelicci (European Institute of Oncology, Milan) and Dr. Scott Lowe (Cold Spring Harbor Laboratories, New York), respectively. The construct encoding p66shc is isoform specific and cannot be spliced to generate the other two isoforms of the adaptor proteins, p46 and p52. The p66shc^{aa} (p66^{Shc}E132Q-E133Q) redox-inactive mutant in the pBabe/Puro backbone was a kind gift of Dr. Fabio Martelli (Molecular Cardiology Laboratory, IRCCS-Policlinico San Donato, Milan, Italy).

To generate the MT-rxYFP-Puro construct from rxYFP cDNA (gift of Dr. Jakob Whinther, Copenaghen, Denmark), the mitochondrial targeting peptide of Cytochrome Oxidase IV was inserted in frame 5′ of the rxYFP start codon in the pcDNA3 vector backbone. The all cassette was then excised and cloned in the retroviral pLPC vector between the BamH1 and XhoI restriction sites.

Plasmids were transfected in the 293-T *Phoenix* Ecotropic packaging cell line (provided by Dr. G. Nolan, University of Stanford, Palo Alto, California) by the Calcium Phosphate precipitation method or the Effectene transfection reagent (Qiagen), and supernatants were used to infect 3T3-L1 preadipocytes in the presence of 4 μg/mL Polybrene (Sigma-Aldrich), as previously described.

The plasmid encoding a GST–PI3Kinase(2SH2) fusion protein in the pGEX vector (Amersham Pharmacia) was a gift of Dr. Kathrine Siminovitch (Mount Sinai Hospital, Toronto, Canada).

The preadipocytic cell line 3T3-L1 was purchased from the Istituto Zooprofilattico della Lombardia e della Emilia Romagna (IZLER, Brescia, Italy). All lines were routinely maintained Dulbecco's Modified Eagle's Medium (DMEM) containing 4.5 g/L glucose (Eurobio) and supplemented with 10% FCS (Sigma-Aldrich and Eurobio), and a mixture of penicillin-streptomycin, pyruvate, glutamine, and nonessential amino acids (Eurobio). Cells were incubated at 37 °C in a humidified CO_2 incubator (5% CO_2 + 95% air).

P66shc Knockdown in 3T3L1 Cells. P66shc-specific and scrambled siRNA duplexes were transfected in 3T3L1 cells using the HiPerFect transfection reagent (Qiagen) according to the manufacturer's recommendations with slight changes. Cells were seeded in complete medium (500 μL) at 50–60,000/well in 12-well plates 16 h before transfection. Transfection (25 nM siRNA) was repeated three times, every 24 h. Protein down-regulation was verified by anti-p66shc immunoblotting.

A 1:1 pool of two different 21mer siRNA specific for mouse p66shcA (accession AK155158.1) was used:

Oligo A(sense): 5′-UGAGUCUCUGUCAUCGCUG*tt*-3′;
Oligo B(sense): 5′-AGGAAAGGCUGCUGAAGAU*tt*-3′.

Bioelectrical Impedance Analysis (BIA) was performed using a tetrapolar electrode arrangement, in which a constant alternating current (0.8 mA) at a fixed frequency of 50 kHz is applied along the length of the body between a pair of electrodes, the voltage drop along the conductor being measured between a second pair of electrodes placed proximally to the current injection electrodes. Resistance (Rz) and Reactance (Xc) values for each mouse were collected over three subsequent determinations, using a commercial body impedance analyzer (BIA 101; Akern) adapted to small animals by the insertion of an additional resistor of 500 Ohm.

MSC adipocytic differentiation. Primary preadipocytes (mesenchymal stem cells, MSCs) purified from the fat of obese p66KO and p66WT mice and propagated for one to three passages were seeded at 10^5 cells/well in 6-well cluster plates (Cornig Life Sciences). in DMEM 20% FCS. At day 2 after confluence medium was changed with fresh DMEM containing the differentiation mix [1 μg/mL insulin, 0.5 mM 1-methyl-3-isobuthyl-xanthine (IMX), 1 μM dexamethasone]; after 2 d differentiation mix was removed and substituted with DMEM + 1 μg/mL insulin, until day 10 (1). Triglyceride accumulation was visualized by Oil Red O staining, as described (1).

Analysis of nutrient and insulin signaling in vitro. Adipocyte precursors propagated for 1–3 passages were seeded at 10^5 cells/well in 12-well cluster plates (CornigLife Sciences). in DMEM 20% FCS. After 16 h, cultures were switched to serum-free DMEM lacking glucose for 5 h. During the last hour of incubation glucose (4.5 g/L) was added.

Adipocytes freshly isolated from inguinal fat pads were resuspended in serum-free DMEM (≈2 g starting material/mL DMEM), stimulated with 250 ng/mL insulin (50 nM) for 20 min and immediately dissolved in lysis buffer.

3T3L1 cells were serum starved overnight and switched to nutrient-depleted DMEM (no glucose, no FCS) for 5 h, before refeeding with 4.5 g/L glucose for 30', 100 ng/mL insulin for 10 minutes, or both. In some experiments 3T3L1 cells were starved in serum-free medium containing 4.5 g/L glucose and directly stimulated with insulin or IGF1 (100 ng/mL) for 10 minutes.

Induction of insulin resistance in vitro. Insulin desensitization of preadipocytes was induced by overnight exposure to excess free fatty acids, according to Nguyen et al. (2) with modifications. MSC cells were treated with a mixture palmitate (500 μM), linoleic (300 μM), and oleic acid (150 μM) in 2% (20 mg/mL) BSA or 2% BSA as control, in serum-free medium. After 16 h, cells were challenged with 100 ng/mL (20 nM) insulin, for 10 minutes for biochemical analysis.

Glucose uptake assay. Glucose uptake by p66WT and p66KO adipocytes in response to insulin was determined according to Olefsky, with slight changes (3). Briefly, cells were isolated from inguinal fat pads of overnight-starved mice, washed twice in PBS, resuspended

in glucose and serum-free DMEM containing 250 ng/mL insulin or vehicle alone, and incubated for 1 h at 37 °C. During the last 3 min of incubation 0.1 mM 2-deoxyglucose and 1 μCi/mL 2-deoxy-D-[1-^{3}H] glucose were added. To remove excess radioactivity, 500 μL of cell suspension were centrifuged on a cushion of 200 μL silicone oil at 10,000 g, and adipocytes were recovered from the top of the oil and lysed in 0.4 mL of 3% SDS. ^{3}H-glucose uptake was determined by scintillation counting. Nonspecific deoxyglucose uptake, as measured in the presence of 20 mM cytochalasin B, was subtracted from the total uptake.

Flow cytometry studies. Cell size and generation of ROS. Cells was analyzed with a 3-fluorescence flow cytometer (488-nm argon laser; COULTER-Epics). For cell size comparisons preadipocytes were fixed in cold Ethanol, permeabilized with Triton X-100 and stained with Propidium Iodide to identify and exclude dividing cells. G1 cell populations were gated and Forward Scatter (FS) profiles compared. ROS generation in glucose refed cells was assessed using the oxidation-sensitive, cell-permeant dye Dichloro-dihydro Fluoresceine-Diacetate (4). Green fluorescence histograms were collected on live [high forward scatter (FS), low side scatter (SS)] cells.

Biochemical studies. For protein phosphorylation studies cells cultured in standard medium unless otherwise indicated were lysed in ice-cold lysis buffer (NaCl 150 mM, Tris-Hcl 50 mM pH 8; 2 mM EDTA) containing 1% vol/vol Triton X-100, 0.1% vol/vol SDS, 1:1,000 protease inhibitor mixture (Sigma), 1 mM sodium orthovanadate, 1 mM NaF; 2 mM β-glycerophosphate. After 15 min on ice with occasional vortexing, cells were spun down at 14,000 rpm, 4 °C to remove debris and unlysed cells, and supernatant quantified for protein content (DC Protein Assay, Biorad), resuspended in 6× Laemmli buffer, boiled, and subdued SDS/PAGE electrophoresis.

For immunoprecipitation (or coimmunoprecipitation) studies, cells/tissues were lysed in low detergent (0.2% Nonidet P-40) buffer and lysates were precleared with empty protein G-sepharose 4B beads (Sigma) before being challenged with specific or control antisera and fresh protein G matrix. After 3 h incubation at 4 °C with continuous agitation, protein-G bound immunocomplexes were collected by centrifugation (14,000 rpm, 30 s) and washed six times in immunoprecipitation buffer. Beads were finally resuspended in 40 μL of 1× Laemmli buffer and boiled. Eluted proteins were subjected to SDS/PAGE and immunoblotting. For GST–PI3K 2(SH2) pull-down assays protein lysates (1 mg) were precleared with empty glutathione-sepharose beads and challenged with 1–2 μg of GST–PI3K fusion protein purified from bacterial lysates by standard procedure. Incubation and washes were performed as for standard immunoprecipitations (5).

Adipose tissue was homogenized in lysis buffer (0.2 g/mL) without detergents with a Ultra-Thurrax homogenizer (Janke and Kunkel), three strokes of 15 s each; Triton X-100 (1% vol/vol) and SDS (0.1% vol/vol) were subsequently added to complete protein extraction. After 15 min on ice, samples were processed as described above. Protein phosphorylation was detected by phosho-specific immunoblotting. In some experiments autoradiographies were digitalized and band intensities quantified by the Quantity One imaging software (Biorad).

Determination of adipocyte size. Inguinal fat pads from representative animals were fixed, included in paraffin, and stained with hematoxylin-eosin by standard procedure. The area of at least 50 adipocytes per mouse from different microscopic fields was determined on digitalized images, using the NIS-Elements Basic Research 2.10 imaging software.

1. Zhang H, et al. (2003) Insulin-like growth factor-1/insulin bypasses Pref-1/FA1-mediated inhibition of adipocyte differentiation. *J Biol Chem* 278:20906–20914.
2. Nguyen MT, et al. (2005) JNK and tumor necrosis factor-alpha mediate free fatty acid-induced insulin resistance in 3T3-L1 adipocytes. *J Biol Chem* 280:35361–35371.
3. Olefsky JM (1978) Mechanisms of the ability of insulin to activate the glucose-transport system in rat adipocytes. *Biochem J* 172:137–145.
4. Bedogni B, et al. (2003) Redox regulation of cAMP-responsive element-binding protein and induction of manganous superoxide dismutase in nerve growth factor-dependent cell survival. *J Biol Chem* 278:16510–16519.
5. Pani G, Fischer KD, Mlinaric-Rascan I, Siminovitch KA (1996) Signaling capacity of the T cell antigen receptor is negatively regulated by the PTP1C tyrosine phosphatase. *J Exp Med* 184:839–852.
6. Maulucci G, et al. (2008) High-resolution imaging of redox signaling in live cells through an oxidation-sensitive yellow fluorescent protein. *Sci Signal* 1:pl3.
7. Giorgio M, et al. (2005) Electron transfer between cytochrome c and p66Shc generates reactive oxygen species that trigger mitochondrial apoptosis. *Cell* 122:221–233.

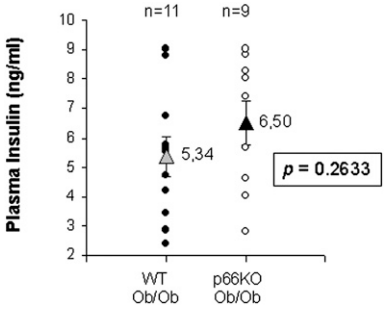

Fig. S1. Plasma insulin levels in obese p66WT and p66KO mice fed ad libitum. Filled (p66WT) and open (p66KO) circles are individual mice, whereas triangles and error bars indicate, for each series, mean ± SEM (5.34 ± 0.66 for p66WT and 6.50 ± 0.76 for p66KO, $P = 0.2633$, difference nonsignificant). *N* values are indicated.

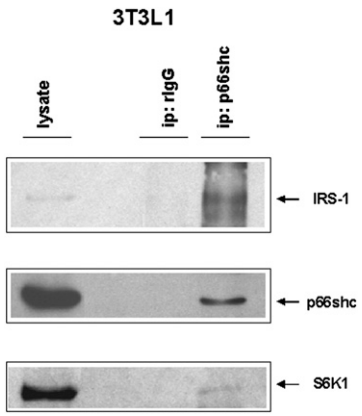

Fig. S2. p66shc and S6K1 physical association in 3T3L1 cells. Endogenous S6K1 and IRS-1 were detected in anti p66shc immunocomplexes but not in a mock immunoprecipitate (rabbit IgG). Protein lysate (1/50 of the total imput lysate) was run in lane 1 and immunoblotted with the same antisera as a positive control. Representative of two independent experiments.

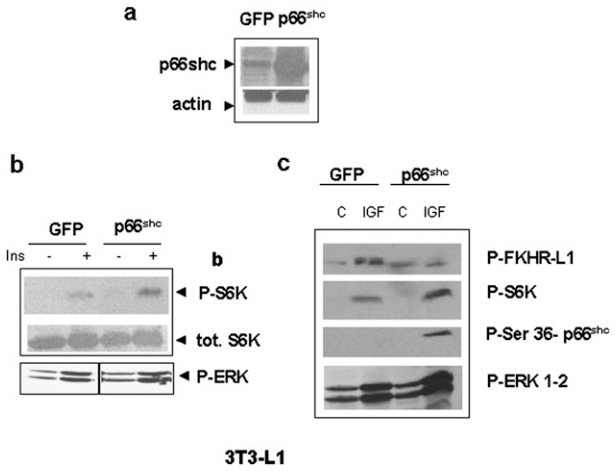

Fig. S3. P66shc amplifies insulin and IGF1 signaling to S6K1. (*A*) Anti p66shc immunoblot analysis confirming up-regulation of the p66shc cell content in retrovirally transduced 3T3-L1 cells. (*B*) Phospho-specific immunoblotting for S6 kinase reveals increased S6K1 response to insulin in undifferentiated 3T3-L1 preadipocytes overexpressing p66shc. (*C*) GFP- and p66-transduced 3T3L1 were stimulated with 100 ng/mL IGF1 for 10 min in serum-free medium. Cell lysates were subdued to SDS/PAGE, transferred onto nitrocellulose membrane, and decorated with the indicated antibodies. Relevant bands are indicated. P66 affects IGF signaling to S6K1 but not to ERK nor to FKHRL-1. P66shc is phosphorylated on Ser-36 in response to IGF1. Picture representative of several independent experiments.

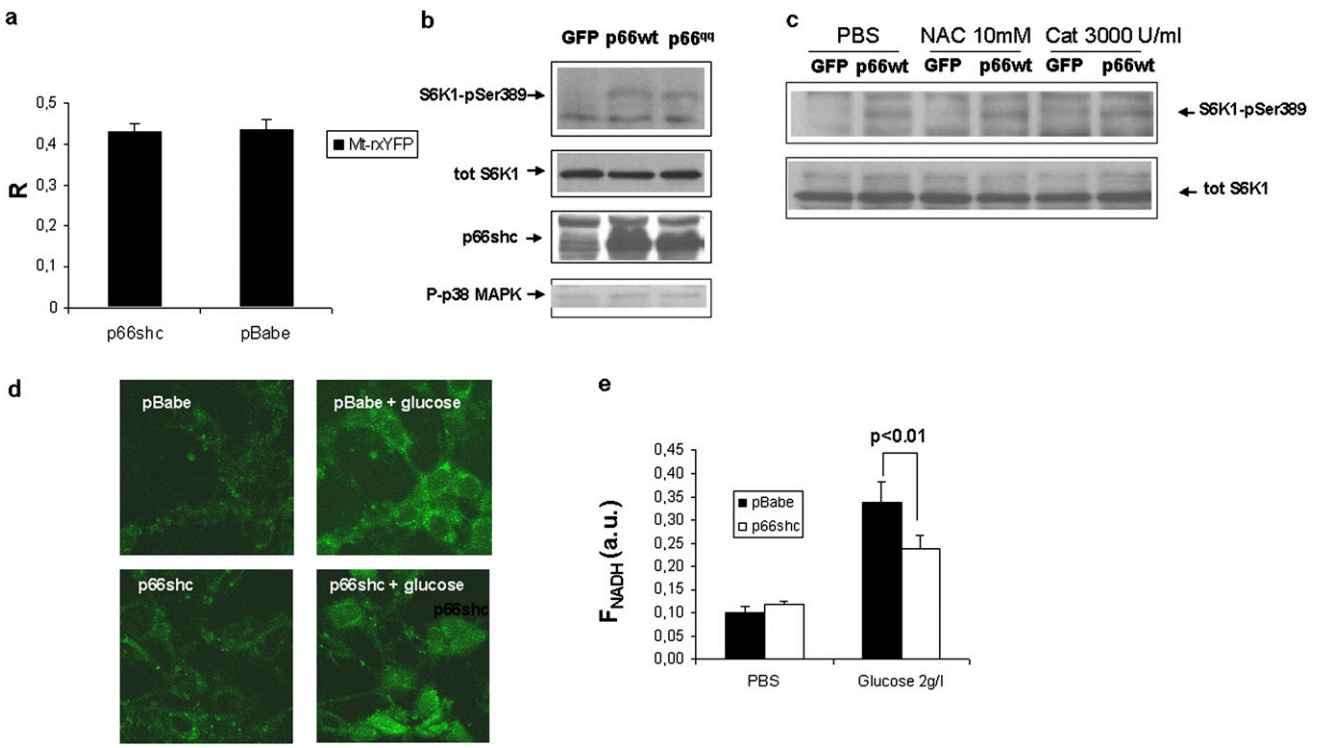

Fig. S4. Effect of p66shc on mitochondrial ROS and intracellular NADH. (*A*) P66shc overexpression does not induce mitochondrial oxidative stress in 3T3L1 preadipocytes. Intracellular redox state of cells coinfected with viral constructs encoding for mitochondrially targeted rxYFP (Mt-rxYFP) and for p66shc (or the corresponding empty vector) and deprived of serum for 2 h was monitored by confocal microscopy, and changes in cell fluorescence calculated ratiometrically as described in ref. 6. *R* is a parameter expressing the distribution of rxYFP between the oxidized (low *R*) and reduced (high *R*) states. Values are mean of 8–9 cells ± SD. Representative of several independent experiments. (*B*) Immunoblot analysis of 3T3L1 cells transduced with retroviral constructs encoding p66shc or a p66shc mutant ($p66shc^{qq}$) reportedly devoid of redox activity (7). Bands corresponding to phosphorylated S6K, phosphorylated p38 MAPK, and total p66shc are indicated by arrows. Equal protein loading was confirmed by anti total S6K staining. Picture representative of two independent experiments. (*C*) Effect of ROS scavengers *N*-acetylcysteine and catalase on S6K phosphorylation by p66shc. Bands corresponding to phospho S6K and total S6K are indicated by arrows. (*D*) Representative microspectrofluorometric images of NAD(P)H accumulation in nutrient-starved 3T3L1 cells after 30 min exposure to glucose. (*E*) Quantitation of NAD(P)H fluorescence from 8 to 10 cells from each condition. Values are mean ± SD of cell fluorescence normalized for the ROI area. Statistical significance, where indicated, was calculated by two-way ANOVA followed by Tukey HSD post hoc test.

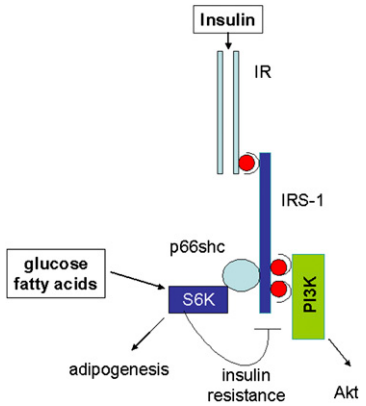

Fig. S5. A model illustrating the major findings of the work. By recruiting S6K to IRS-1 p66shc promotes adipogenic signaling by insulin through the mTOR/S6K pathway, but enhances the S6K-dependent retroinhibitory feedback leading to insulin resistance. The possibility that p66shc promotes S6K activation and its inhibitory action on IRS-1 in response to excess nutrients (glucose and FFA), based on findings from Fig. 4 *A*, *B*, and *F*), is also indicated.